Positron Annihilation Lifetime Spectroscopy (PALS) for Interdiffusion Studies in Disperse Blends of Compatible Polymers: A Quantitative Analysis

G. Dlubek,*,† J. Pionteck,‡ V. Bondarenko,§ G. Pompe,‡ Ch. Taesler,‡,|| K. Petters,§ and R. Krause-Rehberg§

ITA Institute for Innovative Technologies, Köthen, Branch Office Halle, Wiesenring 4, D-06120 Lieskau, Germany, Institute of Polymer Research, Hohe Strasse 6, D-01069 Dresden, Germany, Martin-Luther-University, Department of Physics, D-06099 Halle/S., Germany

Received March 22, 2002; Revised Manuscript Received May 28, 2002

ABSTRACT: Positron annihilation lifetime spectroscopy (PALS) and differential scanning calorimetry (DSC) were used to study the interdiffusion in a particle−matrix system consisting of the miscible polymers poly(vinyl chloride) (particles) and poly(*n*-butyl methacrylate) (matrix, 30:70 and 50:50 w/w). Starting from the demixed state of the blends, the transition to the mixed state during annealing at 110 °C was investigated. We deliver further evidence that PALS parameters such as the orthopositronium intensity I_3 and the average positron lifetime τ_{av} respond to chemical inhomogeneities in blends and their disappearance due to mutual diffusion of molecules of both phases. The response is due to inhibition of Ps formation by one of the constituents when its molecules migrate into the phase made from the second one. A core−shell model for the description of the o-Ps response to a local chemical inhomogeneity is developed which makes use of a calculated concentration−distance profile. The comparison with the experiment allows the estimation of the interface width and of kinetic parameters, such as the exponent of the time dependence of the interface width and the coefficient of mutual diffusion. The potential and the limitation of this new technique are discussed.

Introduction

The interdiffusion in miscible or immiscible polymer blends has been the subject of many investigations and is of interest for several applications like welding and blending of polymers.[1−3] Polymer interdiffusion was studied employing different techniques such as small-angle neutron scattering (SANS), specular neutron reflectivity (SNR), secondary ionization mass spectrometry (SIMS), forward recoil spectroscopy (FRES), attenuated total reflection infrared spectroscopy (ATR−IR), nuclear reaction analysis (NRA), nuclear magnetic resonance (NMR) and direct nonradiative energy-transfer experiments (DET) (see refs 1−3 and references given therein). Most of the techniques are useful for studying the mutual diffusion across the interface between planar double layer polymer films. SANS, NMR, and DET are most appropriate when one has droplets of the labeled polymer dispersed in an unlabeled matrix. The techniques mentioned are sensitive to different types of contrasts, in different length scales and therefore for different stages of interdiffusion.

Recently,[4] we supplied first evidence that positron annihilation lifetime spectroscopy[5,6] (PALS) can be employed for studying the mutual diffusion of polymer molecules in initially demixed blends of inherently miscible polymers. The system investigated consisted of particles of styrene-maleic anhydride copolymer with maleic anhydride content of 24 wt % embedded in a poly(methyl methacrylate) matrix. The PALS results were compared with those obtained from the differential scanning calorimetry (DSC). On the basis of a very simple model, and using results from PALS and conventional DSC experiments, we developed relations for estimating the effects of interdiffusion on the fractional volume of the interfacial interphase.

PALS is nowadays an established technique to study the size of atomic and sub nanometer-sized holes in various materials.[5−10] In amorphous polymers, these holes appear due to the structural (static or dynamic) disorder and constitute the (excess) free volume.[11] A large series of homo- and copolymers has been investigated previously employing PALS. These studies included the investigation of hole sizes in polymer blends as a function of the composition or heat treatment (see refs 12−19 as examples).

The structure of polymers on atomic and molecular level is usually concluded from the value of the orthopositronium (o-Ps) lifetime (τ_3).[7,8] The o-Ps intensity I_3, however, which mirrors the Ps formation probability,[6] may contain essential information on the chemical nature and on possible chemical inhomogeneities of the material in which Ps annihilates.[4,6,13] As we have mentioned already, we have shown recently that the variation of I_3 might be used to study the kinetics of mixing of systems consisting of chemically different polymers.[4] The advantages of the positron/Ps annihilation techniques are the following: (i) The contrast on which these techniques are based differs from that of other methods. (ii) The typical positron annihilation techniques use low cost devices in laboratory scale. (iii) Using conventional positron annihilation techniques, such like PALS or the doppler-broadening of annihila-

* To whom correspondence should be addressed. Telephone: +49-345-5512902. Fax: +49-40-3603241463. E-mail gdlubek@aol.com.
† ITA Institute Köthen/Halle.
‡ Institute of Polymer Research, Dresden.
§ University of Halle.
|| Current address: Eppendorf Polymere GmbH R&D, Barkhausenweg 1, D-22339 Hamburg, Germany.

10.1021/ma020451z CCC: $22.00
Published on Web 07/04/2002

tion radiation (DBAR), polymer blends having a three-dimensional morphology may be studied. (iv) By means of a slow positron beam combined with the DBAR technique[20,21] and the PALS technique,[22] it is possible to investigate model systems of thin planar layers.

In this paper. we continue our work on the application of the PALS technique for the study of interdiffusion phenomena in polymer blends. We improve upon previous work in the following ways: (i) We select a demixed blend system of miscible polymers, which shows much stronger variation in the o-Ps yield I_3 than those previously investigated. (ii) We develop a qualified model for the description of the o-Ps response on local chemical inhomogeneities which makes use of a realistic model function for the concentration−distance profile. This model allows a quantitative analysis of the interdiffusion experiments and the estimation of kinetic parameters. (iii) We discuss in more detail potential and limits of this new method, in particular effects due to a variable coefficient of mutual diffusion.

The system under investigation in this work consists of the two thermodynamically miscible polymers poly(vinyl chloride) (PVC) and poly(*n*-butyl methacrylate) (PnBMA). As a model system for demixed blends we prepared a particle−matrix morphology consisting of fine PVC particles (30 or 50 wt %) embedded in a PnBMA matrix. The interdiffusion process that occurs during annealing of the blends at temperatures above the T_g of both polymers was examined with PALS and DSC. To obtain information on the terminal state of the system, a series of molecularly mixed blends was studied.

Experimental Section

Materials, Sample Preparation, and Characterization. Poly(vinyl chloride) (PVC, Aldrich, $\eta = 0.51$, catalog # 38.929−3) and poly(*n*-butyl methacrylate) (PnBMA, Polysciences, $\eta = 0.50$, $T_g = 20$ °C, catalog # 02061) were precipitated from THF solution into methanol before use. To obtain fine PVC powder the PVC was dissolved again in THF and then dropwise added to *n*-heptane under vigorous stirring. After that the PVC dispersion was treated for 90 min with an ultra sonic finger under cooling in an ice bath, the powder was filtered off, and the remaining *n*-heptane was slowly evaporated under ambient conditions. The powder was dried in a vacuum at 50 °C for 16 h before use. The molecular weights after precipitation determined by GPC were $M_w/M_n = 63\,000/32\,000$ (PVC, PVC standard) and $M_w/M_n = 205.000/103.000$ (PnBMA, PS standard).

Two PVC/PnBMA blends were studied having a composition of 30:70 and 50:50 w/w which corresponds, due to the different densities of PnBMA and PVC ($\rho = 1.048$ and 1.379 g/cm^3, respectively,[23] to volume fractions $v_{PVC} = V_{PVC}/V = 0.246$ and 0.435. The demixed state of blends was obtained by kneading very fine PVC powder into a gel like mass of PnBMA, which contained about 10 wt % *n*-heptane. During kneading and following drying the *n*-heptane evaporates completely. Consequently, the PnBMA was converted into the matrix which contained embedded PVC particles. The material was pressed at 600 MPa and 70 °C to form pills in the size of 1.1−1.4 mm in thickness and 13 mm in diameter. Homogeneously (molecularly) mixed blends containing 5, 15, 30, and 50 wt % PVC were obtained by solution casting from THF. These blends were formed into pills by pressing under the same conditions given above. For studying the interdiffusion process by PALS, the demixed blends were annealed at 110 °C, above the T_gs of the blend components, for various times between 3 and 100 min in an external furnace under argon gas atmosphere conditions.

The particle diameter of the PVC powder was estimated by scanning electron microscopy (SEM) and atomic force microscopy (AFM) and by determination of the specific surface by BET (adsorption isotherm according to Brunauer, Emmett, and Teller) analysis. For SEM a drop of a diluted PVC dispersion in *n*-heptane was put onto a sample holder covered with a double-face conductive tape. After evaporation of the heptane the powder was glued to it. The powder morphology was observed by a Zeiss DSM 982 Gemini with an acceleration voltage of 1 kV for pure powders or 10 kV for powders sputtered with gold. For AFM studies by means of a NanoScope IIIa Dimension 3100 (Digital Instruments) the blends were cut to a pyramid shape and then the tip of the pyramid was cryo cut to obtain smooth surfaces in the size of ca. 0.5×0.5 mm^2. In the tapping mode, the topography and the stiffness contrast have been detected. The BET analysis was carried out by means of an Autosorb-1 (Quantachrome) with nitrogen as adsorbent at 77.4 K.

The DSC measurements were performed with a DSC 7 (Perkin-Elmer), Pyris software Version 3.51 in the temperature range from −30 to +110 °C. The temperature was calibrated with In and Pb standards using a heating rate of 10 K/min. The glass transition behavior was investigated in cycles of heating at a rate of 40 K/min and then cooling at a rate of 80 K/min. The heat flow of the second heating was used for analysis. The high heating rate of 40 K/min was chosen to keep the thermal annealing during the DSC scan as small as possible. In the Pyris version the sample temperature will be recorded, and so the thermal lag at 40 K/min is small (about 1.5 K). For DSC investigation of interdiffusion, the initially demixed blends were annealed inside the DSC between the heat−cool cycles, whereby the annealing temperature was kept constant at 110 °C and the annealing time was stepwise increased from 0.1 min up to 30.3 min (30:70 w/w blend) or up to 300 min (50:50 w/w blend).

Positron Annihilation Lifetime Spectroscopy (PALS). Positron lifetime experiments were carried out at room temperature using a fast-fast coincidence system[5,6] with a time resolution of 228 ps (full width at half-maximum (fwhm)), a channel width of 51.0 ps, and a 1×10^6 Bq ^{22}NaCl positron source sandwiched between two Al foils of 2 mg/cm^2 thickness. To increase the accuracy of the lifetime parameters, five measurements—each lasting 2 h and containing $\sim 8 \times 10^6$ counts—were performed for each of the specimens. A first analysis applying the routine MELT[24] delivered the evidence that all of the spectra consists of three well-separated lifetime components. Employing finally the routine LIFSPECFIT,[25] the lifetime spectra were decomposed (after subtracting background and source components) into three discrete exponentials $s(t) = \Sigma(I_i/\tau_i) \exp(-t/\tau_i)$ ($\Sigma I_i = 1$; $i = 1-3$: para-positronium (p-Ps), free positrons (e^+), and o-Ps annihilation,[6] respectively) having the lifetimes τ_i and intensities I_i. During final fitting, we constrained the p-Ps lifetime to its average of $\tau_1 = 150$ ps and the para-to-ortho Ps intensity ratio to its theoretical value[6] of $I_1/I_3 = {}^1/_3$. Following previous works,[26,27] this procedure delivers most relevant lifetime parameters and decreases distinctly their statistical scatter.

The lifetime parameters and the time-zero channel of the different runs for one specimen always agreed with each other within the statistical error limits of the experiment. In this way the reproducibility of the results was confirmed. Effects which could be due to radiation damage of samples caused by the fast positrons,[28] such as a change in I_3, were not observed. The parameters obtained for the 2 h spectra were averaged to obtain the final results. These results agreed with those analyzed from a spectrum which was obtained by summing the counts of the 5 individual spectra ($\sim 40 \times 10^6$ coincidence counts in total).

Results and Discussion

State of the Demixed Blends and its Change During Annealing. To quantify the interdiffusion across an interface in a heterogeneous bulky particle−matrix system it is necessary to know the interfacial area. However, this interface is hidden and can be

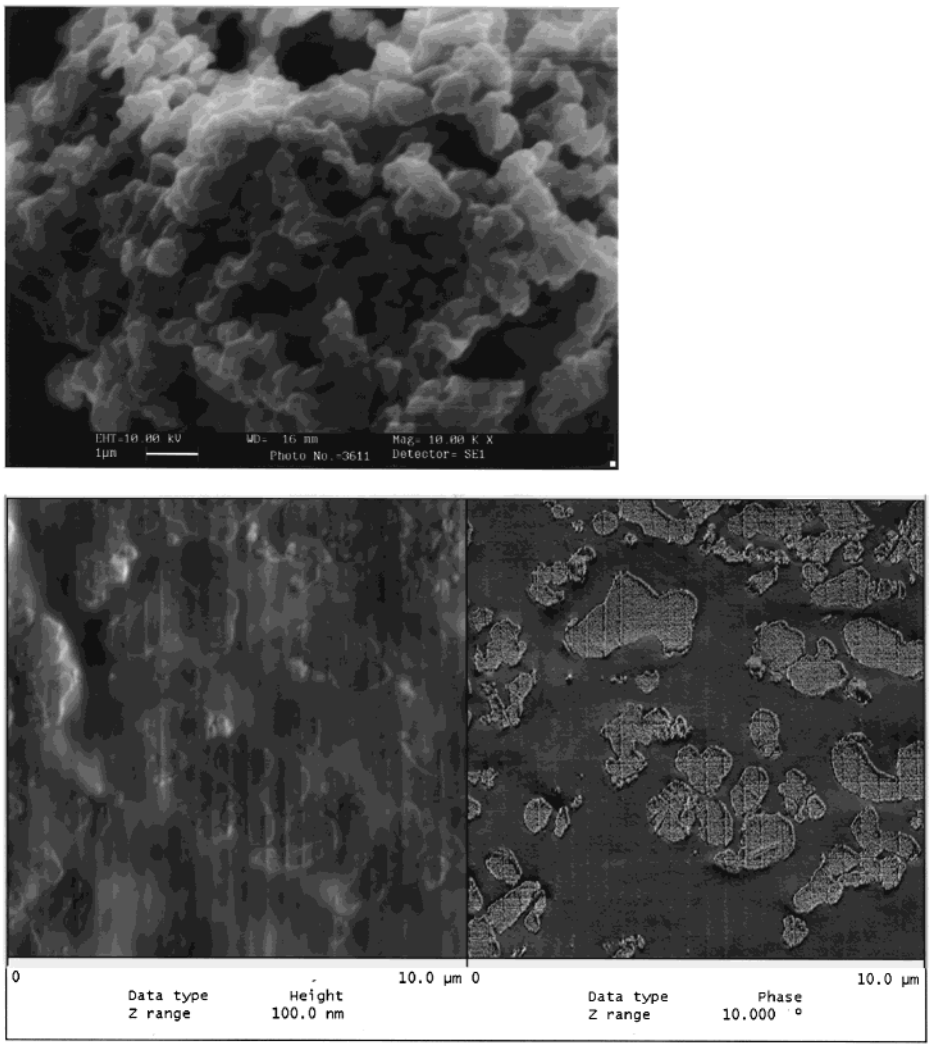

Figure 1. Morphology of PVC particles: (a) on top, SEM of precipitated PVC powder; (b) at the bottom, AFM of a surface cut of the PnBMA/PVC = 30:70 w/w blend, initial state; left, height image; right, phase contrast.

estimated only indirectly. First we determined the specific surface area of the precipitated PVC powder by BET analysis. The average value from three measurements was 31.3 m^2/g, which corresponds to a mean particle diameter of 140 nm. A direct observation of the powder by SEM shows that the particles are strongly agglomerated. Independent of the SEM technique used (with or without sputtering with gold), we always observed big agglomerates consisting of interconnected particles in the size range ca. 300−800 nm (Figure 1a). Because of the continuous like morphology of the agglomerates, a more detailed quantification of the size was not possible.

The morphology of the blends could be evaluated by AFM. In the phase contrast image (Figure 1b, right) one can clearly distinguish the two phases: hard PVC particles and the soft PnBMA matrix. The AFM allows a semiquantitative evaluation of the interfacial area between the matrix and the (partially agglomerated) particles. As in the SEM studies the particle−particle interfaces within the agglomerates are not visible. In the 30:70 w/w blend the size distribution of the PVC phase ranges from about 60 to 1500 nm. From the particle size distribution a number-average particle diameter of 420 nm was estimated. Assuming a spherical shape of the dispersed particles, a surface area average particle diameter of 496 nm was calculated. This value for the effective interfacial area seems to be reasonable considering the BET value and the observed agglomeration. Thus, for the further calculations, we used an mean particle diameter of 450 nm. Because of the lower interparticular distance in higher filled particle matrix systems the agglomeration in the 50:50 w/w blend should be stronger than in the 30:70 w/w system. Therefore, the results obtained for this system should be considered with caution.

Parts a and b of Figure 2 show the influence of the annealing at 110 °C on the heat flow for both blend compositions. The glass transition temperatures of the pure PnBMA and PVC were measured (with a heating rate of 40 K/min) to be 38 and 84 °C, respectively. For comparison with the annealed demixed blends the heat flow of the pure polymers and of the demixed (calculated for the 50:50 w/w blend) and the mixed state are plotted. We can observe that the change of the glass transition behavior reflects the progressive mixing of the blend as consequence of the mutual diffusion of molecules of both constituents with increasing annealing time. The completely mixed state, as it is obtained by solvent casting, is not realized even after 30 or 300 min for the 30:70 and 50:50 w/w blend, respectively. A quantitative analysis of the DSC results will be presented in a separate work.

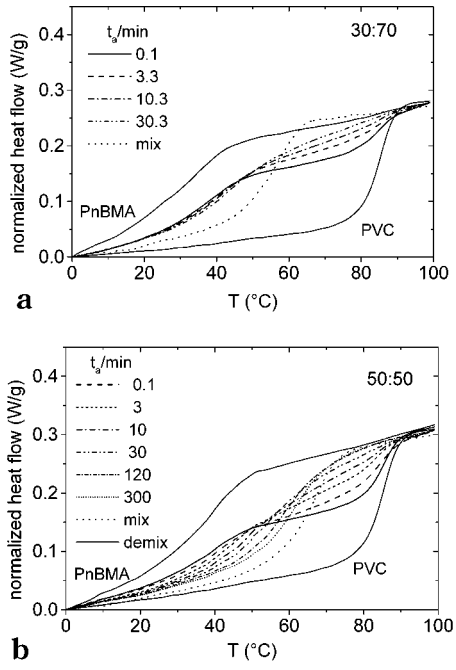

Figure 2. Heat flow curves of the pure components of the blends, the molecularly mixed blends (both second heating), and the particle−matrix (demixed) blends after stepwise annealing at 110 °C within the DSC for different times t_{ann}. The curves for the demixed state of the 50:50 w/w blend were calculated from the scans for the pure polymers. PVC/PnBMA (w/w) = (a) 30:70 and (b) 50:50.

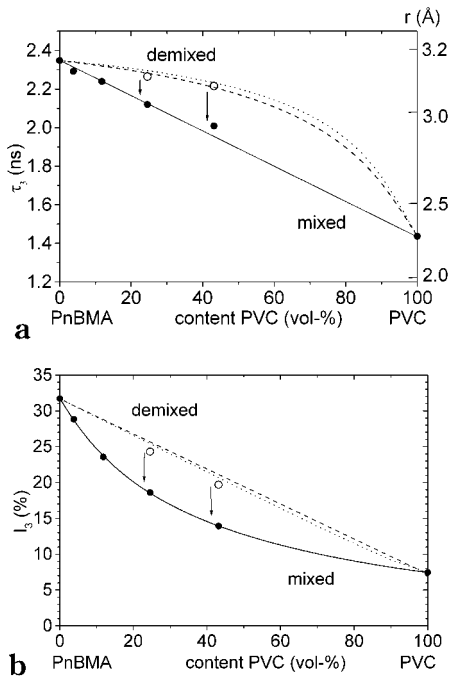

Figure 3. (a) Variation of the o-Ps lifetime τ_3 (left axis) and the free volume hole radius r estimated from τ_3 (right axis) as a function of composition in molecularly mixed (filled symbols) and demixed (particle−matrix) blends (empty symbols) of PVC and PnBMA. Key: dashed line, approximation of eq 1; dotted line, from simulated spectra (see text); solid line, linear fit to the data of the mixed blends. The uncertainties of the experimental data in this and in the following Figures, so far not shown, are smaller than the datum point sizes. (b) As in part a, but with the o-Ps intensity I_3. Here the solid line represents the two-exponential fit to the datum points of the mixed blends (eq 2).

Behavior of PALS Parameters. The three-component analysis of lifetime spectra delivered lifetimes τ_i and relative intensities I_i of 150 ps/2.5−10.6% (p-Ps), 330−360 ps/58−90% (e^+), and 1437−2348 ps/7.5−31.7% (o-Ps). In Figure 3, parts a and b, the o-Ps lifetime τ_3 and the corresponding intensity I_3 of the mixed and demixed polymer blends are shown. The parameters are plotted as a function of the volume fraction of PVC, assuming that there is no change in the molecular volume due to mixing. This was confirmed by pressure−volume−temperature (*PVT*) experiments. When annealing a heterogeneous PnBMA/PVC blend for 5 h at a pressure of 10 MPa at 110 °C within a closed *PVT* cell (PVT Apparatus of Gnomix), the specific volume of the blend was constant within 0.1%.

The o-Ps lifetimes, τ_3, of PnBMA and PVC are 2348 and 1437 ps, respectively. The corresponding o-Ps intensities are 31.73% and 7.45%. The statistical uncertainties of the experiments delivered by the LIFSPECFIT routine are ±3 ps for τ_3 and ±0.04% for I_3. Since additional random errors of different origin may appear, we estimate as realistic uncertainties (standard deviations) ±10 ps for τ_3 and ±0.1% for I_3.

The o-Ps lifetime, τ_3, correlates with the mean size of local free volumes (sub-nanometer size holes) in the amorphous polymer which show a size and a shape distribution. o-Ps atoms are localized within these holes and annihilate during one of their frequent collisions with the hole walls. This process, called pick-off annihilation where the positron in the o-Ps annihilates with a molecular electron of opposite spin, reduces the o-Ps lifetime from 142 ns in vacuo, to about 1−5 ns in polymers. The smaller the hole, the faster the pick-off and the shorter the o-Ps lifetime. Assuming spherical holes their mean radius can be calculated from τ_3 according to a semiempirical model.[7,8] From the values of τ_3, mean hole radii of $r = 3.157 \pm 0.01$ Å for PnBMA and 2.262 ± 0.01 Å for PVC are calculated, these correspond to mean hole volumes of $v = 131.8 \pm 1$ and 48.1 ± 1 Å^3, respectively, (see right-hand axis of Figure 3a). The distinctly larger hole size in PnBMA may be attributed to the side groups of the butyl methacrylate molecule which prevent effective packing of chains. This also causes a high mobility of the main chain which can be observed as lower glass transition temperature compared with PVC.

The o-Ps lifetime τ_3 of the molecularly mixed PnBMA-PVC blend follows almost the straight line obtained from a linear interpolation between the lifetimes of PnBMA and PVC (Figure 3a). That means that no extra local free volume appeared (or disappeared) in the mixed blends which could be attributed to special attractive or repulsive interaction between PnBMA and PVC molecules. The o-Ps lifetimes of the 30:70 and 50:50 (w/w) initial demixed particle−matrix systems are distinctly larger than those of the corresponding molecularly mixed samples. Assuming a linear superposition of the parameters coming from the particles and the matrix, the o-Ps lifetime and its intensity should follow the relations[4,12]

$$\tau_{3,\mathrm{demix}} = [v_p I_{3,\mathrm{PVC}}\tau_{3,\mathrm{PVC}} + (1\text{-}v_p)I_{3,\mathrm{PnBMA}}\tau_{3,\mathrm{PnBMA}}]/I_{3,\mathrm{demix}} \quad (1a)$$

$$I_{3,\mathrm{demix}} = v_p I_{3,\mathrm{PVC}} + (1 - v_p)I_{3,\mathrm{PnBMA}} \quad (1b)$$

Here $v_p = V_p/V$ is the fractional volume of the PVC particle phase, and V_p and V denote the volume of the particle phase and the total sample volume. As can be

observed in Figure 3a, the experimental $\tau_{3,\mathrm{demix}}$ follows closely eq 1a (dashed line). The predictions of eq 1a also behave very similarly to the parameters obtained from analyzing spectra which were generated by the superposition of spectra of the pure polymers weighted with their volume fraction in the demixed blends (dotted line). It appears therefore, that no extra free volume appeared which could be attributed to interfaces;[15,20] this can be interpreted as being due to the compatible nature of both polymers forming the blend.

The o-Ps intensities I_3 of the two demixed blends appear somewhat below the linear relation eq 1b (dashed line in Figure 3b) and also below the values analyzed from generated spectra (dotted line). Two different reasons could cause this effect. First, the preannealing of the system at 70 °C, performed during pressing the sample pills for the formation of the matrix, could lead to dissolution of PVC at the particle−matrix interface and a migration of dissolved PVC molecules into the PnBMA matrix. The DSC experiments performed immediately after pressing of samples and after short time annealing at 110 °C gave some hints that this process take place but with small intensity. As a second reason, the o-Ps intensity may not follow exactly the local variation of composition at the particle−matrix interface, at least for the initial demixed state of the blends. A net flow of Ps or Ps precursors from the matrix to particles may cause the observed effects. Because of the small mean diffusion length of o-Ps and Ps precursors in amorphous polymers determined to be 1−2 nm[28] and 3−10 nm,[28,29] respectively, we estimate that this effect is not very strong, but may explain the observed deviation of I_3 from the linear approximation eq 1b.

The o-Ps intensity of the molecularly mixed blends decreases in a convex curve from $I_3 = 31.73\%$ for pure PnBMA to 7.45% for pure PVC. This nonlinear behavior can be attributed to an inhibition[6,14,19] of the Ps formation caused by the PVC molecules. The o-Ps intensity mirrors the Ps yield P, $I_3 = 3P/4$. Excess electrons are created as consequence of the ionization of molecules by the fast positrons emitted from the ^{22}Na source. In the terminal spur of the positron track the excess electrons may either recombine with ionized molecules, be trapped by scavengers, or form Ps.[6] Inhibition of Ps formation typically occurs when scavengers for excess electrons and/or positrons appear which may then remove these free particles from the Ps formation process.

It is well-known that in liquid or solid solutions chlorine containing groups are very effective Ps inhibitors.[6,30−32] Frequently, this effect is attributed to a dissociative electron capture by a RCl complex followed by the formation of a [Cl^-,e^+]-like bound state.[5,30−32] This type of bound state is expected to have a lifetime of 300−400 ps[33] which corresponds to the value of τ_2. A strong Ps inhibition was observed in polymers, for example, in chlorinated polystyrene[31] and in polycarbonate on addition of *p*-$C_6H_4Cl_2$.[32] We assume that PVC molecules diffused into the PnBMA matrix affect only the Ps yield, but do not react with already formed Ps. In the case of a reaction with Ps (chemical quenching[6]), a lowering of τ_3 below the weight-averaged values is expected which is, however, not observed. This conclusion is in agreement with observations of other authors.[31,32]

The behavior of the o-Ps intensity in a solution showing inhibition is typically described by the empirical relation[6] $I_{3,\mathrm{sol}} = I_3^* + \Delta I_3/(1 + \kappa C^\beta]$ where I_3^*, ΔI_3, κ, and β are fitting constants. Here C is the concentration of scavengers (typically given in mol/volume unit). κ is the inhibition constant which describes the increased interaction of positrons or excess electrons with scavengers compared with other molecular groups. This increased interaction is the physical reason for the nonlinear behavior of $I_{3,\mathrm{mix}}$.

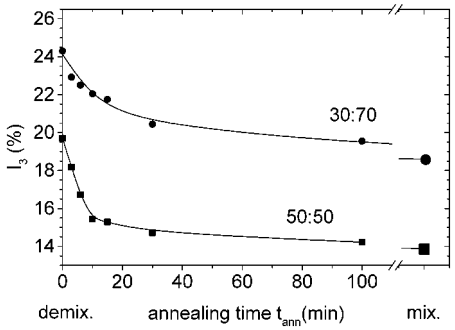

Figure 4. o-Ps intensity I_3 as a function of the annealing time at 110 °C, t_{ann}, for the 30:70 and 50:50 w/w blends. The values for the mixed state (large symbols) were measured on the molecularly mixed samples.

For the quantitative analysis of our interdiffusion experiments we need an analytic function which describes the variation of I_3 of the mixed PVC−PnBMA blends as a function of their composition. This does not have to be the above-mentioned inhibition relation, which has some disadvantageous properties for our application, but can be any other analytical function which describes well the composition dependence of I_3. Best least-squares fits were obtained using a sum of two exponentials as fitting function,

$$I_{3,\mathrm{mix}}(c_{\mathrm{PVC}}) = A_0 + A_1 \exp(-c_{\mathrm{PVC}}/c_1) + A_2 \exp(c_{\mathrm{PVC}}/c_2) \quad (2)$$

where

$$I_{3,\mathrm{mix}}(c_{\mathrm{PVC}} = 0) = I_{\mathrm{m}} = A_0 + A_1 + A_2$$

$$I_{3,\mathrm{mix}}(c_{\mathrm{PVC}} = 1) = I_{\mathrm{p}} = A_0 + A_1 \exp(-1/c_1) + A_2 \exp(-1/c_2)$$

Here, c_{PVC} is the PVC content of the mixture given in fractional volume units. The solid line in Figure 3b shows the best-fit curve which corresponds to the parameters $A_0 = 2.85\%$, $A_1 = 20.04\%$, $A_2 = 8.91\%$, $c_1 = 0.6769$, and $c_2 = 0.1493$.

The average positron lifetime[5,6] $\tau_{\mathrm{av}} = \Sigma I_i \tau_i$ ($i = 1-3$) which is dominated by the term $I_3\tau_3$ shows a behavior similar to that shown by I_3. In the demixed blend, τ_{av} behaves somewhat below the linear approximation eq 1b, while in the mixed system it is well described by an equation corresponding to eq 2.

During annealing of particle−matrix systems at 110 °C the sample state changes from the demixed state toward the mixed state due to the diffusion of molecules from particles into the matrix and vice versa. As a consequence of this, the o-Ps intensity decreases on an exponential-like curve from $I_{3,\mathrm{demix}}$ toward $I_{3,\mathrm{mix}}$ when plotted as a function of annealing time t_{ann} (Figure 4). Analogously, the average positron lifetime τ_{av} and also the o-Ps lifetime τ_3 (not shown) change from the value of the demixed samples toward the value characteristic for the molecular mixture. The behavior of I_3 suggests

that interdiffusion in initially demixed polymer blends, which leads to the decrease in and finally disappearance of chemical inhomogeneity, affects the o-Ps intensity I_3 or another suitable annihilation parameter such as τ_{av} (or the DBAR line shape parameter[5,6]) when one component of the system causes inhibition of Ps formation in the other component.[4] This effect we are going now to utilize for obtaining quantitative information on the kinetics of the interdiffusion process.

Quantitative Analysis of PALS Experiments. For a quantitative analysis of the PALS experiments we assume that the demixed blend consists of spherical particles distributed randomly in the matrix. A spherical core−shell model may describe this disperse system: A particle of radius r_p is located in the center of a spherical cell and surrounded by a shell made from the matrix material. The cell representing the whole system has the radius $r_c = r_p/v_p^{1/3}$. In the completely demixed system the local PVC concentration changes at the particle−matrix interface abruptly from $c_{PVC}(r) = 1$ to 0. We assume that the o-Ps intensity follows this variation and changes in a step from I_p for $0 \le r \le r_p$ to I_m for $r_p < r \le r_c$ (For simplicity we omit the subscript '3' in I_3 and 'PVC' in the local concentration $c_{PVC}(r)$ in the following.). We assume that I_p and I_m are identical with the values observed for the pure particle and matrix materials, $I_p = I_{PVC}$ and $I_m = I_{PnBMA}$. Applying this assumption, the o-Ps intensity of the demixed system corresponds to the volume-weighted average of the particle and matrix intensities as described by eq 1b.

The annealing of the initially demixed system leads to the evolution of spatial distributions of the PVC $c(r)$ and PnBMA $(1 - c(r))$ concentration and in that way also of the o-Ps intensity $I(r)$. The o-Ps intensity-radius profile $I(r)$ at a time t_{ann} of annealing of the initially demixed blend may be described within the core−shell model by

$$I(r) = I_m + (I_p - I_m)F(c(r)) \tag{3}$$

where $F(c(r))$ is the normalized o-Ps intensity profile which is a function of the local concentration $c(r)$ and therefore also of the radius r. The $c(r)$ is given in volume fraction and it is assumed that no volume change occurs during mutual diffusion (incompressibility condition).

The variation of F with the composition of the mixed PVC−PnBMA system may be estimated from experiments using

$$F(c_{PVC}) = \frac{I_{mix}(c_{PVC}) - I_{PnBMA}}{I_{PVC} - I_{PnBMA}} \tag{4}$$

Here $I_{mix}(c_{PVC})$ is the o-Ps intensity in a completely mixed system for a PVC (volume) content of c_{PVC}. It may be described by eq 2. In eq 4, we have defined F in such a way that it varies similarly to the local PVC concentration, i.e., $F(c = 1) = 1$ and $F(c = 0) = 0$.

Similarly to eq 1, the total o-Ps intensity of a particle−matrix system subjected to annealing may be described as the volume average of the local intensity $I(r)$

$$I_{ann} = \frac{3}{r_c^3}\int_0^{r_c} I(r)r^2\,dr \tag{5}$$

From this and eq 3, follows for the relative change of the o-Ps intensity during annealing

$$\Delta I^r_{ann} = \frac{I_{ann} - I_p}{I_m - I_p} = 1 - \frac{3}{r_c^3}\int_0^{r_c} F(r)r^2\,dr \tag{6}$$

For practical purposes, we have defined ΔI^r_{ann} in such a way that it varies similarly to I_{ann}, i.e., $\Delta I^r_{ann} = 1$ for $I = I_m(c = 0)$ and $\Delta I^r_{ann} = 0$ for $I = I_p(c = 1)$. For completely demixed or mixed particle−matrix systems it follows that $\Delta I^r_{ann} = 1 - (r_p/r_c)^3 = 1 - v_p$ and $\Delta I^r_{ann} = 1 - F(c = v_p)$.

In our previous work,[4] we have shown that, assuming a simple three-phase model, the fractional volume of the interfacial phase affected by interdiffusion corresponds to the relative change of the o-Ps intensity I_3 (or any other suitable annihilation parameter). For a more qualified quantitative analysis of the PALS data, one has to use, however, a more realistic model function for describing the concentration−radius profile and its change due to interdiffusion. This function should involve the finiteness of the core−shell system, its radial symmetry, and a possible concentration dependence of D. D is the coefficient of mutual diffusion which controls the rate of disappearance of the concentration gradient in the particle−matrix system moving toward homogeneity.[1] To proceed with the analysis, we first use the solution of the Fickian laws of diffusion (D = constant) in spherical polar coordinates for a finite source of radius r_p embedded in infinite surroundings, assuming that the diffusion is radial (Crank,[34] p 27),

$$c(r) = \frac{1}{2}\left\{\operatorname{erf}\frac{r_p - r}{\sqrt{2}\sigma} + \operatorname{erf}\frac{r_p + r}{\sqrt{2}\sigma}\right\} - \sqrt{\frac{1}{2\pi}}\frac{\sigma}{r}\left\{\exp\left(-\frac{(r_p - r)^2}{2\sigma^2}\right) - \exp\left(-\frac{(r_p + r)^2}{2\sigma^2}\right)\right\} \tag{7}$$

As previously, the concentration $c(r) = c_{PVC}(r)$ is given in volume fraction and $c_{PVC}(r) + c_{PnBMA}(r) = 1$ is valid. In eq 7, erf(z) is the well-known error function[34] which has the properties erf(0) = 0, erf(∞) = 1, and erf(−z) = −erf(z). σ is the standard deviation of the error function and may be considered as a parameter which corresponds to half of the width of the interface layer affected by the interdiffusion. It is related to D via

$$\sigma = (2Dt_{ann})^{1/2} \tag{8}$$

where t_{ann} is the annealing time.[34] Equation 7 satisfies the initial conditions ($t_{ann} = 0$) $c = 1$ for $0 \le r \le r_p$ and $c = 0$ for $r_p < r \le r_c$, as well as the boundary condition of no material flux $\partial c/\partial r = 0$ for $t_{ann} > 0$ at $r = 0$. For values smaller than $\sigma \approx (r_c - r_p)/3$, the values of c and $\partial c/\partial r$ at the cell boundary $r = r_c$ are sufficiently small to satisfy the law of material conservation within the cell.

For larger values of σ, eq 7 does not satisfy the boundary condition $\partial c/\partial r = 0$ at $r = r_c$ for $t_{ann} > 0$, and material flows out of the cell. Therefore, we use for these values of σ a numerical solution of Fickian equation. Using the finite-difference method (see Crank,[34] p 197) the concentration $c_{m,n+1}$ at the grid point $r = m\,dr$ at the annealing time $t_{ann} = (n + 1)\,dt$ (m = 1, 2, 3, ...; n = 0, 1, 2, 3, ...) can be estimated from those at time $t_{ann} = n\,dt$ via

$$c_{m,n+1} = c_{m,n} + \frac{M}{m}[(m-1)c_{m-1,n} - 2c_{m,n} + (m+1)c_{m+1,n}] \quad (9)$$

with $M = D\,\mathrm{d}t/(\mathrm{d}r)^2$. For the numerical calculation we started with the analytical solution eq 7 for $\sigma = 0.08\ r_p$ and used $M = {}^1/_2$ and $\mathrm{d}r = r_c/100$. $\mathrm{d}t$ is then given by $\mathrm{d}t = (r_c/100)^2/2D$ and σ for $\sigma > 0.08$ by $\sigma = (n + 100)^{0.5} r_c/100 r_p$. The boundary conditions were satisfied by assuming $c_{0,n+1} = c_{1,n}$ and $c_{100,n+1} = c_{99,n}$.

In Figure 5, the concentration profiles c for $\sigma/r_c = 0$, 0.1, 0.3, and 0.6 are shown as examples. $v_p = 0.25$ has been assumed. With increasing σ (or annealing time t_{ann}) the gradient in the concentration in the vicinity of $r = r_p$ disappears gradually, and the concentration profile moves toward homogeneity. The calculations satisfied the mass conservation, estimated from $c_{PVC}^{cell} = (3/r_c^3)\int c(r) r^2\,\mathrm{d}r$ $(r = 0 \ldots r_c)$, $c_{PVC}^{cell} = v_p$, always within 10^{-3}. Figure 5 shows also the normalized local intensity function $F(c(r))$. It can be observed that F is always larger than $c = c_{PVC}$ due to the inhibition of the Ps formation by PVC molecules diffusing from particles into the PnBMA matrix. At $t_{ann} > 0$ the difference between the values of $c(r)$ and $F(r)$, integrated over the whole volume of the cell, controls the decrease of the o-Ps intensity below the initial value I_{demix} measured at $t_{ann} = 0$.

The relative change of the o-Ps intensity, ΔI^r_{ann} (see eq 6), due to interdiffusion calculated for a particle−matrix system with $v_p = 0.246$ (corresponding to our 30:70 w/w blend) is plotted in Figure 6 for increasing values of σ. ΔI^r_{ann} decrease from a value of $\Delta I^r_{ann} = 1 - v_p = 0.754$ for $\sigma = 0$ (demixed state) toward 0.454 for $\sigma \rightarrow \infty$ (completely mixed state). For small values of σ, $0 \le \sigma/r_c \le 0.20$, the decrease is almost linear; it flattens distinctly for larger σ. For $\sigma \approx 0.4/r_c$, ΔI^r_{ann} approaches the value of the completely mixed state and shows no further sensitivity to the interdiffusion process. As can be estimated in Figure 5, the concentration−radius profile is already very flat for such large values of σ. The ΔI^r_{ann} curve for a particle−matrix system with $v_p = 0.435$ (corresponding to 50:50 w/w) shows a similar behavior (Figure 6). It decreases from $\Delta I^r_{ann} = 0.565$ for $\sigma = 0$ to 0.244 for $\sigma \rightarrow \infty$. Since for this blend $(r_c - r_p)/r_c$ is smaller than for the blend with $v_p = 0.246$, the linear decrease of ΔI^r_{ann} ranges only up to $\sigma/r_c \approx 0.15$.

Effect of a Variable Diffusion Coefficient on the Data Analysis. In the above analysis, we assumed that the diffusion coefficient is constant. This must be considered, however, as a strong simplification. The mutual diffusion in miscible blends of chemically different polymers depends on both frictional and thermodynamic interactions among the molecules of the system, and therefore, it is generally dependent on the composition of the system.[1,2,35,36] These effects complicate the analysis of experimental data and will affect our results. We will, therefore, investigate the consequences of having a variable diffusion coefficient in this chapter. In doing this, we assume a certain concentration dependence of the interdiffusion coefficient, construct the corresponding concentration−radius profile, and study how the annihilation parameters change.

It is known that the diffusion coefficient increases with the temperature following the Vogel−Tamman−Fulcher equation, or, equivalently, the Willam−Landel−Ferry (WLF) equation.[36−38] Within a limited temperature range, D exhibits an exponential behavior. In

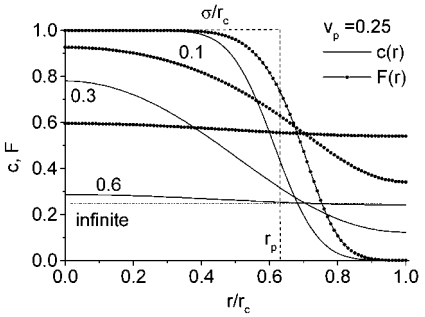

Figure 5. Concentration−radius profile $c(r)$ calculated for different values of interfacial width parameter σ and the normalized local intensity function $F(c(r))$ as a function of the radius in a spherical core−shell cell describing the disperse system. A volume fraction of the dispersed component of $v_p = 0.25$ was assumed. The particle is located centrally in the disperse system unit cell, and the particle−matrix interface appears initially at $r_p = (0.25)^{1/3} r_c = 0.630 r_c$, where r_c is the radius of the cell.

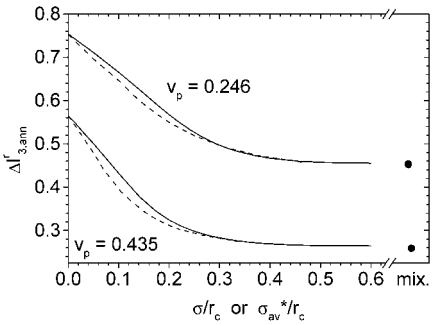

Figure 6. Relative variation of the o-Ps intensity, $\Delta I^r_{3,ann}$, as a function of the (half) interface width σ (σ_{av}*) calculated for two particle−matrix systems with particle fractions of v_p assuming either a constant (solid lines as a function of σ) or an exponential varying (dashed lines as a function of σ_{av}*, see text) diffusion coefficient.

labeled PMMA[37] or in PMMA blends,[38] for example, it increases by approximately 2 orders of magnitude when $T - T_g$ increases from 26 to 72 K. These temperature differences correspond to the difference between our annealing temperature and the glass transition temperature T_g of PVC and PnBMA, respectively. Dielectric relaxation data show that at 110 °C the α relaxation frequencies in PnBMA[39] are higher than in PVC[40] by a factor of about 16.

Since the T_g of the mixed blend to a first approximation depends linearly on the composition c, one can assume an exponential concentration dependence of the mutual diffusion coefficient:[37]

$$\check{D} = \check{D}_0 \mathrm{e}^{a(1-c)} \quad (10)$$

where $\check{D}_0$ and a are constants. In eq 10, we have assumed that the chain mobility dominates the variation of $\check{D}$. For comparison with a constant diffusion coefficient D, we choose $\check{D}_0$ in such a way that the variable diffusion coefficient $\check{D}$ averaged over the range of concentration,

$$\check{D}_{av} = (1/c_0)\int_0^{c_0} \check{D}\,\mathrm{d}c \quad (11)$$

corresponds to D:

$$\check{D}_0 = D\frac{a}{\mathrm{e}^a - 1} \quad (12)$$

With this relation, the corresponding standard deviation σ^* varies with c as

$$\sigma^* = \sigma\left[\frac{a}{e^a - 1}e^{a(1-c)}\right]^{0.5} \tag{13}$$

where σ is related to D via eq 8, and the concentration average of σ^*, σ_{av}^* (calculated from a relation analogously to eq 11), agrees with σ, $\sigma = \sigma_{av}^*$. For $a = 2 \ln 10 = 4.6052$, $\check{D}$ varies exponentially by 2 orders of magnitude, from the mutual diffusion coefficient in almost pure PVC ($c \rightarrow 1$), $\check{D}_{PVC} = \check{D}_0 = 0.0465D$, to the mutual diffusion coefficient in almost pure PnBMA ($c \rightarrow 0$), $\check{D}_{PnBMA} = 100\ \check{D}_0 = 4.652D$. Correspondingly, σ^* changes by 1 order of magnitude, from 0.2157σ to 2.157σ.

For the calculation of the concentration−distance profile, we used an iterative analytical method provided that $\sigma_{av}^* \leq 0.08/r_c$. For larger values of σ_{av}^*, the profile was calculated numerically using the finite-difference method adapted to the exponential dependence of $\check{D}$. To keep this paper as concise as possible, we go without a description of these calculations. The interested reader may consult ref 34, §9.32 and §10.13. In Figure 6, we have plotted the behavior of ΔI^r_{ann} calculated for the variable diffusion coefficient $\check{D}$ described above and also that for a constant D. Since eq 10 assumes a higher diffusivity in the PnBMA-rich regions, more PVC molecules are transported into the outer parts of the cell, and the PVC concentration there grows faster than for a constant D. PnBMA molecules, however, exhibit the opposite behavior and show almost no in-diffusion into the PVC particles, but the particle−matrix interface moves toward the immobile component, i.e., the particles show a shrinkage with increasing annealing time, respectively increasing σ_{av}^*. For a given value of σ_{av}^*, the net effect is a stronger lowering of ΔI^r_{ann} than calculated for the concentration independent σ. For higher values of σ_{av}^*, ΔI^r_{ann} approaches the value of the molecularly mixed state. The data shown in Figure 6 are calculated for the behavior of the o-Ps intensity I_3.

Our results indicate that the annihilation parameters do not depend very strongly on the specific variation of the mutual diffusion coefficient $\check{D}$, but are dominated by its concentration weighted average $\check{D}_{av}$. The reason for this behavior is that the annihilation parameters are integral values which are affected by the whole concentration−radius profile. In fact, the assumption of a parabolic variation of $\check{D}$, enhanced in the middle of the composition range, leads to a ΔI^r_{ann} vs σ_{av}^* curve which lies between both the curves shown in Figure 6. A parabolic variation of $\check{D}$ may appear when the thermodynamic term expressing the deviation from ideal state of mixing dominates the diffusion coefficient.[35−37]

From a comparison of the experimental values of ΔI^r_{ann} with the calculated ones we may now conclude on the value of σ (or σ_{av}^*) which agrees best with the experiment. For this comparison we have normalized ΔI^r_{ann} in such a way that the normalized relative intensity $\Delta I^{r,n}_{ann}$ changes between 1 for the demixed state ($\sigma = 0$) and 0 for the completely mixed state ($\sigma \rightarrow \infty$) independently of the real volume fraction of particles. This normalization simplifies the comparison of the calculated $\Delta I^{r,n}_{ann}$ with those estimated from different experimental quantities and helps to overcome the problem that the experimental parameters of the demixed blends do not agree with the linear approximation eq 1b assumed to be valid in the calculation of the theoretical curves.

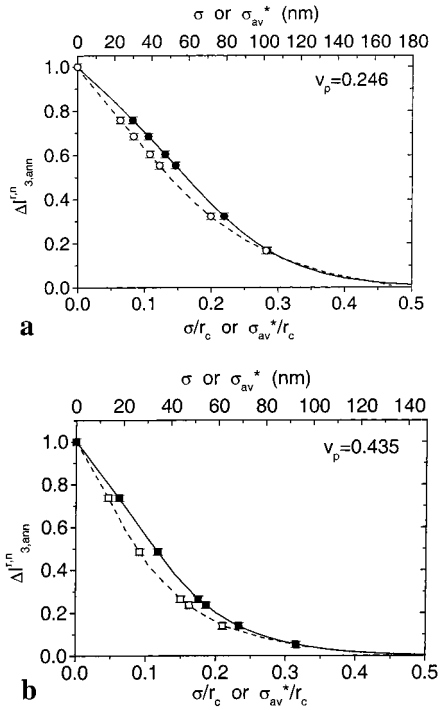

Figure 7. (a) As in Figure 6, but normalized relative variation of the o-Ps intensity, $\Delta I^{r,n}_{3,ann}$ for the 30:70 w/w blend. Key: lines, calculations; symbols, experimental data; filled symbols and solid line, σ; empty symbols and dashed line, σ_{av}^*. (b) As in part a, but for the 50:50 w/w blend.

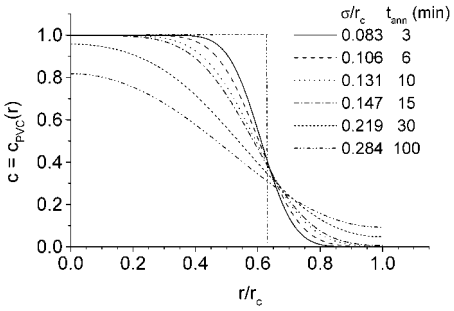

Figure 8. Evolution of spatial distributions of the PVC molecules $c = c_{PVC}(r)$ (in volume fractions) within a repeating cell of radius r_c during the annealing of the disperse 30:70 w/w blend at 110 °C. The values of interfacial width parameter σ were estimated from the data in Figure 7a assuming a constant coefficient of mutual diffusion.

In parts a and b of Figure 7, the calculated values of $\Delta I^{r,n}_{ann}$ are shown as a function of the relative σ/r_c. The absolute values of σ and σ_{av}^* are calculated for a mean particle diameter of 450 nm, as was estimated from the morphology analysis. The experimental values of $\Delta I^{r,n}_{ann}$ were plotted at such values of σ (or σ_{av}^*) that they correspond to the calculation. In this way the values of σ (or σ_{av}^*) corresponding to the experiments may be determined from this figure. Figure 8 shows the evolution of spatial distributions of the PVC molecules, $c = c_{PVC}(r)$, for the 30:70 w/w blend calculated using the values of interfacial width parameter σ which were estimated from the data in Figure 7a (D = constant). With increasing annealing time t_{ann}, PVC molecules move from the particle−matrix interface into the matrix and approach for $t_{ann} \approx 15$ min the cell boundary. Simultaneously, PMMA molecules move into the par-

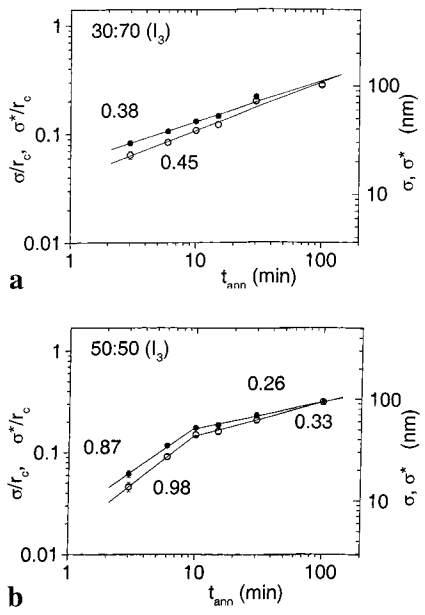

Figure 9. (a) log−log plot of the interface width parameter σ respectively σ^* vs the annealing time t_{ann} for the 30:70 w/w blend. The figures indicate the slope k of the fitted straight lines. Key: filled symbols, σ; empty symbols, σ^*; both estimated from I_3. (b) As in part a, but for data of the 50:50 w/w blend.

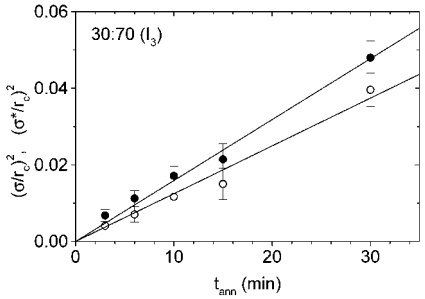

Figure 10. Square of the half interface width (σ, filled circles; σ_{av}*, empty circles; both estimated from I_3) of the 30:70 w/w blend vs the annealing time. From the slope of the straight lines, the coefficient of interdiffusion (D or $\check{D}_{av}$) is estimated (see text).

ticle. For annealing times longer than 15 min, the pure particle and matrix material disappears and the system tends to approach more and more the completely mixed state.

As can be observed in Figure 7, parts a and b, the sensitivity of PALS to the variation of the interfacial width parameter σ ranges from 0 to ∼250 nm for the blend with a volume fraction of particles of $v_p = 0.246$ and from 0 to ∼150 nm for the blend with $v_p = 0.435$. The uncertainty in $\Delta I^{r,n}{}_{ann}$ (standard deviation: 0.015) correspond to uncertainties in σ of 1 nm ($v_p = 0.435$) and 2 nm ($v_p = 0.246$), respectively.

In the following section, we study the kinetic behavior of the interface width parameter σ estimated as described above. One may generalize eq 8 and assume that σ (or σ_{av}*) varies like $\sigma = (\text{constant}) t_{ann}{}^k$ where exponent k is a constant. In parts a and b of Figure 9 σ and σ_{av}* (estimated from I_3) are plotted vs t_{ann} in a log−log scale for the blends under investigation. One can observe that in the 30:70 w/w blend the interfacial mixing proceeds with the same power law within the annealing times applied. A value of $k = 0.38 \pm 0.02$ assuming a constant diffusion coefficient and a somewhat larger one, $k = 0.45 \pm 0.03$, for an exponential variation of the diffusion coefficient were determined. In the case of the 50:50 w/w blend, the slope k is distinctly larger for short annealing times ($k \approx 0.9$ for $t_{ann} \leq 10$ min). The nature of these large values is not clear and may be related to agglomeration and inhomogeneous distribution of PVC particles in this blend. For annealing times longer than 10 min, values of $k = 0.26 \pm 0.03$ and $k = 0.33 \pm 0.03$, respectively, being somewhat smaller than those of the 30:70 w/w blend, were found. Values of $k = 0.25$ are considered to be typical for the Rouse-type motion[41,42] of coupled chain segments.[3] Values of $k = 0.13$ and 0.28 were observed for the early stage of interdiffusion between films of PVC and poly(methyl methacrylate).[43] For later annealing stages Fickian diffusion, $k = 0.5$, is expected to occur.[3]

When assuming tentatively that the diffusion follows the Fickian rules, i.e., $\sigma = (2\, D\, t_{ann})^{0.5}$, one may estimate D from the plot of σ^2 vs t_{ann}, shown in Figure 10. We fitted a straight line, constrained to pass zero, to the data in the limited range $0 \leq t_{ann} \leq 40$ min and obtained a value of $D = (2.6 \pm 0.1) \times 10^{-5}\ r_c{}^2\ s^{-1}$ when plotting σ, and $\check{D}_{av} = (2.0 \pm 0.1) \times 10^{-5}\ r_c{}^2\ s^{-1}$ when plotting σ^*, respectively. With $r_c = 360$ nm for the 30:70 blend ($\langle r_p \rangle = 225$ nm), values of $D = 3.5 \times 10^{-17}$ m^2/s and $\check{D}_{av} = 2.5 \times 10^{-17}$ m^2/s follow. For the 50:50 w/w blend, the plots are highly nonlinear; therefore, the slope was not estimated. The same results as from I_3, within the uncertainties of the experiments, we obtained from data estimated from τ_{av}. Therefore, they are not shown.

In summary, the estimated coefficient of interdiffusion D (or $\check{D}_{av}$) in the 30:70 w/w PVC−PnBMA blend is on the order of $\sim 1 \times 10^{-18}$ m^2/s. Assuming that $\check{D}(c)$ actually shows the assumed exponential variation, boundary values of $\check{D}(c \rightarrow 1) \approx 1.5 \times 10^{-19}$ m^2/s and $\check{D}(c \rightarrow 0) \approx 1.5 \times 10^{-17}$ m^2/s would follow. We must take into account, however, that the numerical value of $\check{D}_{av}$ not only depends on the accuracy of the estimated particle radius but also may be affected by the distribution of particle sizes and by inhomogeneities in the spatial particle distribution. Unfortunately, it is not easy to compare the diffusion coefficient with values from the literature since $\check{D}$ depends on the frictional and thermodynamic interactions among the molecules of the binary system, on the temperature, on the entanglement density, and on the molecular mass and may be also highly concentration dependent. Values of $\check{D}$ between 10^{-17} and 10^{-20} m^2/s depending on the system, composition, and temperature were observed (see Composto et al.[36] and Qiu and Bousmina[44] and references given therein). Jabbari and Peppas[45] estimated the diffusion coefficient $\check{D}$ from mapping the concentration profile across the interface of a PVC/poly(ethyl methacrylate) couple at 100 °C to 8×10^{-17} m^2/s. Similar values were found for the PVC/poly(ϵ-caprolactone) system.[46]

Conclusion

PALS is a useful technique for studying interdiffusion in blends of chemically different polymers. The intensity of the o-Ps annihilation, I_3, and annihilation parameters related to this such as the average positron lifetime τ_{av} and, as we observed also, the DBAR line shape parameter (here not shown) respond clearly to the chemical inhomogeneity of the blend and its change. The response appears when one of the components of the blend causes inhibition of Ps formation in the other component. Polar groups with a high electron affinity such as carbonyl[14]

or nitrile[4,14] groups and chlorine may act as scavengers for free electrons in polymers which in this way are removed from the Ps formation process. Because of the diffusion of polymer molecules containing Ps inhibitors from one phase into another, the integral o-Ps intensity I_3 of the blend is lowered compared with the totally demixed state of the system. This effect can be used for studying the kinetics of the interdiffusion.

Assuming a core−shell model for the description of the o-Ps response to a local chemical inhomogeneity which makes use of a calculated concentration−distance profile, the interface width and kinetic parameters such as the exponent of its time dependence k of the interface width and the coefficient of mutual diffusion $\breve{D}_{av}$ may be estimated. Values of $k = 0.38-0.45$ and $\breve{D}_{av} = (2.5-3.5) \times 10^{-17}$ m^2/s were obtained. We analyzed the DSC data using a similar model to that with which we analyzed PALS measurements. It delivered kinetic parameters ($k = 0.42$, $\breve{D}_{av} = 2 \times 10^{-17}$ m^2/s) very similar to those estimated from PALS. The details of this work will be published in a subsequent paper.

A limitation of the PALS technique is that the concentration dependence of the mutual diffusion coefficient is unknown and therefore difficult to consider correctly during analysis. Our results indicate, however, that the annihilation parameters do not depend very strongly on the specific variation of the diffusion coefficient, but instead, are dominated by the concentration weighted average of the variable coefficient.

The PALS technique may also be used to study the opposite process of mixing, to study the demixing of initially mixed blends, and to determine binodal and spinodal decomposition temperatures, and on the way create a complete phase diagram of a blend. It may be applied not only to engineering polymer blends having a three-dimensional morphology but also for the study of the mutual diffusion across the interface between planar double layer polymer films. For the latter application a monoenergetic slow positron beam in combination with PALS or DBAR will be used. Since the penetration depth of monoenergetic positrons may be varied from some tenths of a nanometer to about 20 μm, the concentration−distance profiles can be scanned systematically. These experiments should deliver more detailed information on the interdiffusion process such as the concentration dependence of the diffusion coefficient, for example. Such studies are currently in progress.

Acknowledgment. The authors wish to thank V. Albrecht for the BET analysis, A. Janke for the AFM images, and D. Voigt for the GPC analysis. C.T, and J.P. are grateful to the Deutsche Forschungsgemeinschaft for financial support (DFG Project Number PI 308/3-1). D. Kilburn/Bristol is acknowledged for critical reading of the manuscript.

References and Notes

(1) Kausch, H. H.; Tirell, M. *Annu. Rev. Mater. Sci.* **1989**, *19*, 341.

(2) Green, P. F. Translational Dynamics of Macromolecules in Melts. In *Diffusion in Polymers*; Neogi, P., Ed.; Marcel Dekker: New York, 1996; p 251.

(3) Stamm, M. Reflection of Neutrons for the Investigation of Polymer Interdiffusion at Interfaces. In *Physics of Polymer Surfaces and Interfaces*; Butterworth Heinemann: Boston, MA, 1992; p 163.

(4) Dlubek, G.; Taesler, C.; Pompe, G.; Pionteck, J.; Petters, K.; Redmann, F.; Krause-Rehberg, R. *J. Appl. Polym. Sci.* **2002**, *84*, 654.

(5) Dupasquier, A.; Mills, A. P., Jr., Eds.; *Positron Spectroscopy of Solids, Proceedings of the International School of Physics "Enrico Fermi", Course CXXV, Varenna, Italy, July 6−16, 1993*; IOOS Press: Amsterdam, 1995.

(6) Mogensen, O. E. *Positron Annihilation in Chemistry*; Springer-Verlag: Berlin and Heidelberg, Germany, 1995.

(7) Eldrup, M.; Lightbody, D.; Sherwood, J. N. *Chem. Phys.* **1981**, *63*, 51.

(8) Nakahishi, N.; Jean, J. C. In *Positron and Positronium Chemistry*; Schrader, D. M., Jean, Y. C., Eds.; Studies in Physical and Theoretical Chemistry 57; Elsevier Sci. Publ.: Amsterdam, 1988; p 159.

(9) Jean, Y. C. *Microchem. J.* **1990**, *42*, 72. See also ref 5, p 563.

(10) Pethrick, R. A. *Prog. Polym. Sci.* **1997**, *22*, 1.

(11) Simha, R.; Somcynsky, T. *Macromolecules* **1969**, *2*, 342.

(12) Maurer, F. H. J.; Welander, W. *J. Adhes. Sci. Technol.* **1991**, *5*, 425.

(13) Wästlund, C.; Schmidt, M.; Schantz, S.; Maurer, F. H. J. *Polym. Eng. Sci.* **1998**, *38*, 1286.

(14) Wästlund, C.; Maurer, F. H. J. *Polymer* **1998**, *39*, 2897.

(15) Wästlund, C.; Berndtsson, H.; Maurer, F. H. J.*Macromolecules* **1998**, *31*, 3322.

(16) McCullagh, C. M.; Yu, Z.; Jamieson, A. M.; Blackwell, J.; McGervey, J. D. *Macromolecules* **1995**, *28*, 6100.

(17) Peng, Z. L.; Olson, B. G.; Srithawatpong, R.; McGervey, J. D.; Jamieson, A. M.; Ishida, H.; Meier, T. M.; Halas, A. F. *J. Polym. Sci., Part B: Polym. Phys.* **1998**, *36*, 861.

(18) Chang, G.-W.; Jamieson, A. M.; Yu, Z.; McGervey, J. D. *J. Appl. Polym. Sci.* **1997**, *63*, 483.

(19) Fang, J.; Tanaka, K.; Kita, H.; Okamoto, K.; Ito, Y. *J. Polym. Sci., Part B: Polym. Phys.* **2000**, *38*, 1123

(20) Krause-Rehberg, R.; Leipner, H. S. *Positron Annihilation in Semiconductors*, Springer-Verlag: Heidelberg, Germany, 1999.

(21) Cao, H.; Zhang, R.; Juan, J.-P.; Huang, C.-M.; Jean, Y. C.; Suzuki, R.; Ohdaira, T.; Nielsen, B. *J. Phys.: Condens. Matter* **1998**, *10*, 10429.

(22) Gidley, D. W.; DeMaggio, G. B.; Frieze, W. E.; Zhu, M.; Hristov, H. A.; Yee, A. F. Positron Annihilation, Proceedings of the 11th International Conference (ICPA-11), Kansas City, MO, May 1997. In *Materials Science Forum*; Jean, Y. C., Eldrup, M.,Schrader, D. M., West, R. N., Eds.; Trans Tech: Ütikon-Zürich, Switzerland, 1997; Vol. 255−257, p 635.

(23) Zoller, P.; Walsh, D. *Standard Pressure−Volume−Temperature Data for Polymers*; Technomic Publishing Co., Inc.: Lancester, PA, and Basel, Switzerland, 1995.

(24) Shukla, A.; Peter, M.; Hoffmann, L. *Nucl. Instrum. Methods* **1993**, *A335*, 310. Hoffmann, L.; Shukla, A.; Peter, M.; Barbiellini, B.; Manuel, A. A. *Nucl. Instrum. Methods* **1993**, *A335*, 276.

(25) LIFSPECFIT 5.1, Lifetime spectrum fit version 5.1, Technical University of Helsinki, Laboratory of Physics, 1992.

(26) Dlubek, G.; Hübner, Ch.; Eichler, St. *Phys. Status Solidi A* **1998**, *168*, 333; *Nucl. Instrum. Methods* **1998**, *B142*, 191.

(27) Dlubek, G.; Eichler, St.; Hübner, Ch.; Nagel, Ch. *Phys. Status Solidi A* **1999**, *174*, 313; *Nucl. Instrum. Methods* **1999**, *B 149*, 501.

(28) Hirata, K.; Kobayashi, Y.; Ujihira, Y. *J. Chem. Soc., Faraday Trans.* **1997**, *93*, 139.

(29) Uedono, A.; Kitano, T.; Hamada, K.; Morija, T.; Kawano, T.; Tanigawa, S.; Suzuki, R.; Ohdaira, T.; Micado, T. *Jpn. J. Appl. Phys.* **1997**, *36*, 2571.

(30) Eldrup, M.; Shantarovich, V. P.; Mogenson, O. E. *Chem. Phys.* **1975**, *11*, 129.

(31) Baranowski, A.; Debowska, M.; Jerie, K.; Mirkiewicz, G.; Rudzinska-Girulska, J.; Sikorski, R. T. *J. Phys. (Paris) IV*, Colloque C4, supplement *J. Phys. (Paris) II*, **1993**, *Colloque 3*, 225.

(32) Hirata, K.; Kobayashi, Y.; Ujihira, Y. *J. Chem. Soc., Faraday Trans.* **1996**, *92*, 986.

(33) Nuramagambetov, S. B. In *Positron Annihilation, Procedings of the 7th International Conference (ICPA-7), New Dehli, India, January 1985*; Jain, P. C., Singru, R. M, Gopinathan, K. P., Eds.; World Scientific: Singapore, 1985; p 770.

(34) Crank, J. *The Mathematics of Diffusion*; Clarendon Press: Oxford, England, 1956.

(35) Johnes, R. A.; Klein, J.; Donald, A. M. *Nature (London)* **1986**, *321*, 161.

(36) Composto, R. J.; Kramer, E. J.; White, D. M. *Macromolecules* **1988**, *21*, 2580.

(37) Veniaminow, A. V.; Sillescu, H. *Macromolecules* **1999**, *32*, 1828.
(38) Xie, J. L.; Wang, C. H. *J. Chem. Phys.* **1991**, *94*, 3229.
(39) Schröter, K.; Unger, R.; Reissig, S.; Garwe, F.; Kahle, S.; Beier, M.; Donth, E. *Macromolecules* **1998**, *31*, 8966.
(40) Ishida, Y. *Kolloid. Z.* **1969**, *168*, 29.
(41) Rouse, P. E. *J. Chem. Phys.* **1953**, *21*, 1272.
(42) Doi, M.; Edwards, S. F. *The Theory of Polymer Dynamics*; Clarendon Press: Oxford, England, 1986.
(43) Kunz, K.; Stamm, M. *Macromol. Symp.* **1994**, *78*, 105.
(44) Qiu, H.; Bousmina, M. *Macromolecules* **2000**, *33*, 6588.
(45) Jabbari, E.; Peppas, N. A. *Polym. Bull. (Berlin)* **1991**, *27*, 305.
(46) Gilmore, P. T.; Falabella, R.; Laurence, R. L. *Macromolecules* **1980**, *13*, 880.

MA020451Z